Integration of Phase-Change Materials with Electrospun Fibers for Promoting Neurite Outgrowth under Controlled Release

*Jiajia Xue, Chunlei Zhu, Jianhua Li, Haoxuan Li, and Younan Xia**

Dr. J. Xue, Dr. C. Zhu, Dr. J. Li, H. Li, Prof. Y. Xia

The Wallace H. Coulter Department of Biomedical Engineering

Georgia Institute of Technology and Emory University

Atlanta, GA 30332, USA

Prof. Y. Xia

School of Chemistry and Biochemistry, School of Chemical and Biomolecular Engineering

Georgia Institute of Technology

Atlanta, GA 30332, USA

E-mail: younan.xia@bme.gatech.edu

This is the author manuscript accepted for publication and has undergone full peer review but has not been through the copyediting, typesetting, pagination and proofreading process, which may lead to differences between this version and the Version of Record. Please cite this article as doi: 10.1002/adma.201705563.

Abstract

We report a temperature-regulated system for the controlled release of nerve growth factor (NGF) to promote neurite outgrowth. The system is based upon microparticles fabricated using coaxial electrospray, with the outer solution containing a phase-change material (PCM) and the inner solution encompassing payload(s). When the temperature is kept below the melting point of the PCM, there is no release due to the extremely slow diffusion through a solid matrix. Upon increasing the temperature to slightly pass the melting point, the encapsulated payload(s) can be readily released from the melted PCM. By leveraging the reversibility of the phase transition, the payload(s) can be released in a pulsatile mode through on/off heating cycles. The controlled release system is evaluated for potential use in neural tissue engineering by sandwiching the microparticles, co-loaded with NGF and a near-infrared dye, between two layers of electrospun fibers to form a tri-layer construct. Upon photothermal heating with a near-infrared laser, the NGF is released with well-preserved bioactivity to promote neurite outgrowth. By choosing different combinations of PCM, biological effector, and scaffolding material, this controlled release system can be applied to a wide variety of biomedical applications.

Keywords: phase-change material • coaxial electrospray • electrospun fibers • controlled release • neural tissue engineering

Table of contents entry

On-demand release for tissue engineering: Microparticles comprised of a phase-change material (PCM), a near-infrared dye, and payload(s) were fabricated using coaxial electrospray. When sandwiched between two layers of electrospun fibers, the payload (*e.g.*, nerve growth factor) could be released upon photothermal heating to promote neurite outgrowth.

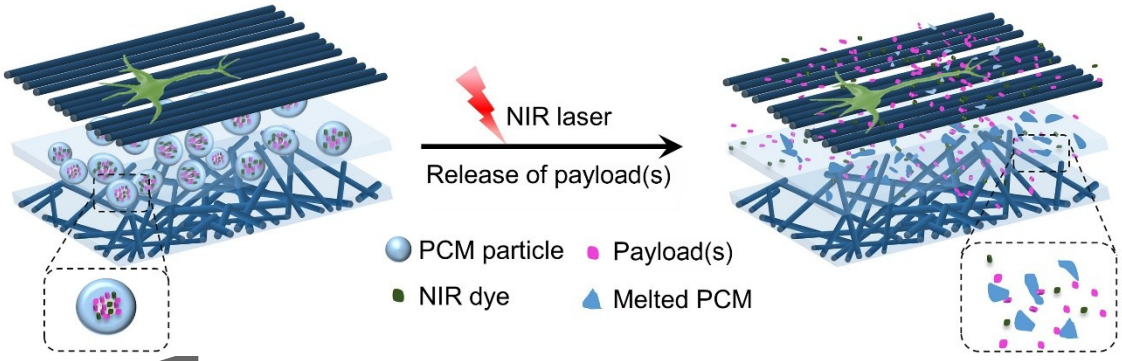

1. Introduction

Electrospun fibers are playing an increasingly important role in a diverse range of biomedical applications, such as tissue engineering, drug delivery, and diagnostics. When integrated with biological effectors and cells, electrospun fibers have shown great promise in interfacing with the neural tissues and promoting axon regeneration.[1,2] In the case of neural interface, electrospun fibers have been loaded with drugs or neurotrophins and then applied as bioactive coatings for neural electrodes[3-5] and as neural implants to enhance the growth of neuronal processes or to reduce the reactive tissue response and gliosis.[6] In the case of nerve repair, electrospun fibers have been collected as uniaxially aligned arrays to direct glial alignment and promote the growth of neurites and axons. Despite the progress, it remains a challenge to place temporal and spatial controls over the delivery of biological effectors such as growth factors during the fabrication of scaffolding materials.[6,7] In general, it is necessary to control and manage the release of growth factors from the scaffolding materials under both *in vitro* and *in vivo* conditions.[8,9] Such a requirement can be easily met by integrating electrospun fibers with a controlled release system based upon a stimuli-responsible material.

Stimuli-responsive materials are able to change conformations and other physicochemical properties upon exposure to an external or internal stimulus.[10] Various types of external stimuli have been explored to trigger the release, including temperature,[11,12] ultrasound,[13] magnetic field,[14,15] electric field,[16,17] and light.[18] Among them, thermo-sensitive materials and photothermal triggering have recently emerged as an attractive means for on-demand release. To this end, near-infrared (NIR) light with deep penetration in soft tissues can be remotely applied with high spatial and temporal precision while causing essentially no damage to cells and tissues at the site of interest.

A number of thermo-sensitive materials have been developed for applications in controlled release.[19] Most recently, phase-change materials (PCMs) have been explored as a

new class of thermo-sensitive materials by leveraging their reversible solid-liquid phase transition in response to temperature variation.[13,19-22] Among the various kinds of PCMs, natural fatty acids are particularly attractive owing to the low cost, as well as high stability, biocompatibility, and biodegradability.[23] Considering that the triggering temperature should have no adverse impact on normal cells and tissues, it is important to use PCMs with melting points close to 37 °C, the physiological temperature of human body. To this end, the melting points of PCMs based upon fatty acids can be readily tuned using mixtures with variable compositions.[24-26] In particular, we recently identified a eutectic mixture of lauric acid and stearic acid to give a single melting point at 39 °C. Both lauric and stearic acids have absolute biocompatibility since they are derived from natural fats. This PCM can serve as a gating material for controlling the generation and release of free radicals to eradicate cancer cells.[27] It can also be adopted to reconstitute the core of low-density lipoprotein to realize metabolism-triggered drug release,[28] and furthermore, be constructed into smart nanoparticles for intracellular drug delivery.[29] The payload can be triggered to release only by photothermally or ultrasonically heating the system to a temperature slightly above 39 °C.

During the fabrication of the aforementioned systems for controlled release, elevated temperatures or organic solvents are typically involved, greatly limiting their use towards applications involving biological effectors such as growth factors and enzymes. Among various fabrication methods,[30,31] electrospray is a versatile and cost-effective technique that has been demonstrated for generating drug-loaded microparticles with a controlled composition, particle size, structure, and morphology from solutions of polymers, ceramics, and small molecules.[32-35] In particular, coaxial electrospray can be applied to directly load a biological effector into the microparticles without compromising the bioactivity by keeping the biological effector separated from the organic solvent.[36,37]

Herein we report a new platform for thermally triggered release of growth factors, which is based upon microparticles fabricated using coaxial electrospray. The microparticles are

made of a PCM, with the core region containing payload(s). The payload is only released from the PCM matrix upon heating to a temperature above the melting point. To evaluate the potential application of this release system in neural tissue engineering, we sandwich the microparticles co-loaded with nerve growth factor (NGF) and a NIR dye between two layers of electrospun fibers to form a tri-layer construct. The outgrowth of neurites is greatly enhanced under the controlled release of NGF. In principle, this controlled release system based upon PCM microparticles can also be extended to other scaffolding materials such as hydrogels or polymer matrices towards a wide variety of tissue engineering applications.

2. Results and Discussion

2.1. Characterization of the Microparticles Fabricated Using Electrospray

We recently developed a PCM with a sharp melting point at 39 °C by mixing lauric acid and stearic acid at a mass ratio of 8:2.[29] Figure S1 shows a differential scanning calorimetry (DSC) curve of the PCM, indicating a single melting point. In the present work, we process the PCM into microparticles loaded with a biological effector in one step through the use of coaxial electrospray (Figure 1A). For the purpose of proof-of-concept, we used Rhodamine B (RB) and fluorescein isothiocyanate labelled bovine serum albumin (FITC-BSA) as the payloads to represent small organic molecules and proteins, respectively. As illustrated by the drawing in the inset, the outer and inner solutions, which are PCM dissolved in an ethanol and dichloromethane mixture and RB dissolved in an aqueous gelatin solution, respectively, are immiscible. During the electrospray process, the PCM precipitates out to form particles while the payload is retained in the core region as the solvents evaporate. Figure 1B shows an optical micrograph of the PCM microparticles loaded with RB. We analyzed the shape of the microparticles by measuring the aspect ratio (AR, defined as the ratio of length to width for

the particle) of these particles (n = 200). About 84% of the PCM microparticles showed a spherical shape, with an average value of 1.09 for the AR).[35] Because of the non-uniform evaporation of solvents and the difficulty in precisely controlling the temperature and humidity of the environment during the electrospray process, some PCM microparticles also took irregular shapes. Figure 1, C and D, shows fluorescence micrographs of the as-obtained particles loaded with RB and FITC-BSA, respectively, confirming the successful encapsulation of these fluorescence dyes inside the particles. As shown by the scanning electron microscopy (SEM) image in Figure 1E, the particles encapsulated with FITC-BSA also displayed a spherical shape, with an average diameter of 5.6 ± 1.8 μm (n = 200) (see Figure S2 for a plot of size distribution). We then quantified the size polydispersity of the particles by calculating the coefficient of variation (CV, defined as the ratio of the standard deviation of diameter to the mean diameter) for the sizes of the particles. The particles exhibited some polydispersity in size, with CV = 32%.[35] For the application explored in this work, the size variation should not cause any negative impact in terms of performance and outcome. We also characterized the distribution of payload in the particles using laser scanning confocal microscopy (LSCM). With RB serving as the payload, as shown in Figure S3, the RB was indeed located in the core region of the as-obtained microparticles. Interestingly, the resultant microparticles could be stably dispersed in water, phosphate buffered saline, and cell culture medium through simply sonication for several seconds, making it easy to incubate them with cells, deposit them onto other substrates, or incorporate them into scaffolding materials.

2.2. Release of Payloads from the Microparticles

The encapsulation efficiencies, defined as the ratio of actually encapsulated amount to theoretical amount, of different payloads in the PCM microparticles were all greater than

80%. The release profile of a payload from the PCM particles was studied by dispersing the particles in deionized water to form a homogeneous dispersion and then holding the system at a temperature below or above the melting point of the PCM. Figure S4A shows the cumulative release of RB from the particles when continuously incubated in a water bath held at 37 °C or 40 °C. At 37 °C, there was only some slight release of RB from the particles. During the coaxial electrospray process, the minor mixing between the inner and outer solutions could result in the deposition of a small amount of RB on or near the outer surface of the particles. In comparison, when the sample was heated to 40 °C, almost 80% of the encapsulated RB was released from the particles within 2 min. As shown in Figure S4B, under a heating/cooling cycles, the RB was released in a pulsatile mode. As indicated by the plots in Figure 2A, the release of FITC-BSA from the particles showed a similar profile, with major release at 40 °C and minor release at 37 °C. The release rate of FITC-BSA from the particles was slightly slower than that of RB because of the higher molecule weight of FITC-BSA and the stronger interaction between FITC-BSA and fatty acids.

We also used horseradish peroxidase (HRP) as a model of biological effector to investigate the release profile and the influence of electrospray on its bioactivity. To avoid the possible loss of bioactivity caused by long-term heating, the sample was only heated at 40 °C for 3 min. After heating in a centrifuge tube, the particles were cooled down in an ice bath and centrifuged, and the supernatant was collected for measurement. The heating/cooling cycles were repeated five rounds. Figure 2B shows the release content of HRP from the particles after each round. During the first cycle of heating, PCM particles melted into liquid, resulting in the release of payload into water. In the cooling process, PCM solidified quickly and a small portion of the released payload would be re-encapsulated and centrifuged down with the PCM solid, leading to the pulsatile release mode. It should be pointed out that after the first cycle of heating the PCM was no longer presented in a particulate morphology.

After the particles had been heated at 40 °C for 3 min, we evaluated the enzymatic activity of the released HRP by tetramethylbenzidine (TMB) colorimetric assay. After reacting with TMB for 20 min, aqueous HCl was added to terminate the reaction, and the absorbance of the reaction product at 450 nm was measured to determine the enzymatic activity. The UV/vis absorption spectra of the blue-colored product derived from the reaction between TMB and the released HRP were monitored continuously every 30 s for 10 min (Figure 2C). The increase in peak absorbance with time suggested the well-preserved activity of the released HRP. Figure 2D shows a comparison with native HRP at the same enzyme concentration of 0.25 nM. The slight reduction in slop in the initial linear region indicated a somewhat reduced enzymatic activity for the HRP released from the particles. Compared with native HRP, the enzymatic activity of the released HRP was 76.5 ± 6.1% of the native enzyme. We can conclude that the payloads could be released from the particles by heating to 40 °C without significantly reducing the activity.

To demonstrate the ability of releasing payloads from PCM particles by photothermal heating, we co-loaded indocyanine green (ICG) into the particles as a NIR absorber. Upon irradiation with a CW diode laser (808 nm) at different power densities, there was a quick temperature rise with time in the dry particles, as illustrated by the plots in Figure S5. When the particles deposited on glass slide and then rinsed with water, the temperature could rise to slightly pass the melting point of the PCM as demonstrated by the infrared images in Figure 3A. At power densities of 1.0 W/cm^2, the temperature could reach 40 °C within only 6 s of irradiation. The temperature rise rate could also be adjusted by varying the amount of ICG encapsulated in the particles. It is important to avoid excessive rise in temperature for the purpose of preserving the bioactivity of the encapsulated biological effector. Figure 3B shows the release profile of FITC-BSA from the particles supported on a glass coverslip, which was immersed in deionized water to receive five rounds of on and off cycles of laser irradiation. At a power density of 1.0 W/cm^2, almost all FITC-BSA was released within five rounds of

irradiation. In contrast, only minor release was detected in the absence of laser irradiation. Compared to direct heating, the same level of cumulative release could be reached for FITC-BSA within a shorter period of time for laser irradiation. This acceleration can be ascribed to the difference in maximum temperature the particles could experience during the two heating processes. In the case of direct heating, the particles were suspended in water in a centrifuge tube and then heated in a water bath. The maximum temperature was set by the temperature of the water bath. For laser-based heating, the particles were deposited on a glass coverslip and then immersed in deionized water, followed by irradiation of the entire surface with the diode laser. Depending on how quickly the heat could be dissipated from the PCM microparticles, the instant temperature experienced by the microparticles could be higher than what was revealed using IR camera, which is based on the average readings over a certain period of time. In addition, even after the laser was turned off, the PCM could still stay in the melted state during the cooling process, allowing the payload to be continuously released.

Upon laser irradiation, HRP was also released from the particles in a pulsatile profile (Figure 3C). After five rounds of laser irradiation, no enzymatic activity was detected any more. We recorded the absorbance at 650 nm for the product derived from TMB and the released HRP upon 6 s of laser irradiation at a power density of 1.0 W/cm^2. As shown in Figure 3D, the absorbance increased with time, suggesting well-preserved enzymatic activity for the released HRP, which was 94.7% ± 4.2% of the native HRP. Meanwhile, only a small amount of HRP was released in the absence of laser irradiation. Thus, it can be concluded that payloads could be triggered to release from the PCM particles under the photothermal effect and the bioactivity of the biological effector was largely preserved.

We then examined the cytotoxicity of the PCM particles at different concentrations ranging from 2–1000 μg/mL using NIH-3T3 cells and cell counting-kit 8 (CCK-8) assay. As shown in Figure S6, the particles showed no obvious cytotoxicity until reaching a high

concentration of 500 μg/mL. This result confirms that the PCM particles can be used as a safe carrier for drug delivery.

2.3 Fabrication of the Tri-layer Construct

The biological effector-loaded PCM particles can be readily incorporated into a scaffolding material for tissue engineering application. Here we integrated the PCM particles containing NGF with mats of electrospun fibers for promoting neurites outgrowth. Combing electrospray with electrospinning, we directly fabricated a tri-layer construct by sandwiching the NGF-loaded PCM particles between two layers of electrospun fibers. One layer was comprised of random fibers to provide mechanical strength, while the other layer was made of uniaxially aligned fibers to provide physical guidance for neurite outgrowth. The different morphologies of the electrospun fibers in the random and aligned layers were confirmed by SEM. As shown in Figure S7, the average diameters of the random fibers and aligned fibers were 1021 ± 46 nm and 923 ± 34 nm (n = 200), respectively. To derive the highest content of PCM particles that could be sandwiched between two layers of electrospun fibers without causing any cytotoxicity, we examined the effect of PCM content on the biocompatibility of the tri-layer construct. We fabricated tri-layer constructs with different PCM contents by setting the duration of electrospray to 5, 10, and 20 min, respectively. We then tested the viabilities of NIH-3T3 cells cultured on the different tri-layer constructs. From Figure S8, the tri-layer construct showed no obvious cytotoxicity when the particles were collected for 5 min. Therefore, we used an electrospray time of 5 min to collect the NGF-loaded PCM particles between two layers of electrospun fibers to fabricate the tri-layer construct for studying neurite outgrowth. As shown in Figure S9, the thickness of the layer consisting of random fibers was 217 ± 19 μm while that of aligned fibers was 196 ± 25 μm. When electrospraying for 5 min, the number of microparticles was not even enough to completely cover the surface

of the underlying mat of fibers, indicating that the layer of PCM particles should have a thickness essentially the same as the diameter of the particles.

2.4 Release of NGF from the Tri-layer Construct

We separately measured the release profiles of NGF from the tri-layer constructs upon direct heating and photothermal heating. In this case, the payload would be released from the melted PCM and then diffused through the electrospun fiber layers to the surrounding medium. This process would take some time to complete, so we used longer exposure durations to ensure the complete diffusion of the payloads from the tri-layer construct. As shown in Figure 4A, when directly heating the construct for 3 min and repeated six rounds, about 52.3 ng of NGF was cumulatively released at 40 °C while only 9.7 ng was released at 37 °C. In this case, the encapsulated content of NGF in the tri-layer construct was about 32.1 ± 2.3 ng/cm^2. The encapsulation content could be easily adjusted by varying the concentration of NGF in the inner solution for electrospraying, the area of the collector, and the electrospray time. When ICG was co-loaded with NGF in the PCM particles, we evaluated the release of NGF from the tri-layer construct upon laser irradiation. Figure 4B shows the cumulative release of NGF from the tri-layer construct upon 6 s of laser irradiation at a power density of 1.0 W/cm^2. The diameter of laser spot at a power density of 1.0 W/cm^2 was about 10 mm, so the amount of the released NGF we detected was only from the area of the construct that was irradiated by the laser. Upon photothermal heating, the PCM melted and the encapsulated NGF diffused out into the surrounding medium through the layers of electrospun fibers.

2.5 Neurite Outgrowth under the Controlled Release of NGF

We examined the activity of the released NGF by investigating the neurite outgrowth from PC12 cells under the stimulation of the NGF released from the tri-layer construct upon direct heating or photothermal heating. For direct heating, the construct was placed in the apical chamber of a 24-well insert and then placed in a well of a 24-well plate in which PC12 cells were cultured at the bottom. Afterwards, the well plate was heated at 40 °C for 3 min at day 0, 2, 4, and 6, respectively. At day 7, the neurite outgrowth from the PC12 cells was examined, as shown in Figure S10. Upon direct heating, the neurites extruded from the PC12 cells under the stimulation of the NGF released from the tri-layer construct, and no significant difference in neurite length was observed when compared with the group of free NGF. In the absence of direct heating, much shorter neurites extruded from the PC12 cells, which can be attributed to the negligible release of NGF from the tri-layer construct at 37 °C. Therefore, the NGF released from the tri-layer construct upon direct heating had well preserved bioactivity and could diffuse into the culture medium to stimulate the neurite outgrowth.

For photothermal heating, we firstly measured the amount of NGF cumulatively released from the tri-layer construct into the culture medium. The construct was placed in the apical chamber of a 24-well insert and then placed in a well of a 24-well plate, followed by the addition of culture medium. Afterwards, the tri-layer construct was irradiated with the diode laser at a power density of 1.0 W/cm^2 for 6 s at day 0, 2, 4, and 6, respectively. At day 7, a cumulative release of 12.7 ± 1.6 ng NGF was detected in the medium relative to 1.9 ± 0.5 ng of NGF in the absence of laser irradiation. These media were then collected for the incubation of PC12 cells to examine the activity of the released NGF. Figure S11 indicates that longer neurites were extended from the PC12 cells when incubated in the medium collected from the group with laser irradiation in comparison with the group without laser irradiation.

We then investigated the outgrowth of neurites from PC12 cells under the controlled release of NGF from the tri-layer construct upon photothermal heating. The PC12 cells were

cultured at the bottom of a well in a 24-well plate. The construct was placed in the apical chamber of a 24-well insert and then placed in the well. Afterwards, the tri-layer construct was irradiated with the diode laser at a power density of 1.0 W/cm^2 for 6 s at day 0, 2, 4, and 6, respectively. At day 7, the neurite outgrowth from PC12 cells was examined. From Figure 5A, when a bi-layer construct, with one layer made of random fibers and the other layer made of aligned fibers, was placed in the insert, no neurites was extended from the PC12 cells. A similar result was observed from Figure 5B when a tri-layer construct sandwiched with ICG-loaded PCM particles was placed in the insert. However, when free NGF were supplemented in the culture media, as shown in Figure 5, C and D, neurites were extended from PC12 cells in both groups, indicating that only in the presence of NGF, PC12 cells could be stimulated to project neurites. Moreover, in the group of tri-layer construct sandwiched with ICG-loaded PCM particles, the average length of the neurites was 18% longer than the group of bi-layer construct. This result indicates that the PCM could promote the NGF-induced neurite outgrowth from PC12 cells. Figure 5E shows the neurites outgrowing from PC12 cells when the tri-layer construct containing NGF was placed in the insert. Upon laser irradiation, neurites extruded from PC12 cells under the stimulation of the NGF released from the tri-layer construct, and no significant difference in neurite length was observed when compared with the group of free NGF. Therefore, upon laser irradiation, NGF could be released from the tri-layer construct with well-preserved bioactivity. In the absence of laser irradiation, as shown in Figure 5F, much shorter neurites extruded from the PC12 cells because essentially no NGF was released from the tri-layer construct. We can conclude that under the synergistical promotion of the released NGF and the PCM, the neurite extension from PC12 cells was greatly enhanced. Under pulsed laser irradiation, we were able to obtain freshly released NGF from the tri-layer construct.

Furthermore, we investigated the outgrowth of neurites from PC12 cells directly cultured on the tri-layer construct under pulsed laser irradiation, as illustrated in Figure 6A. To better

identify and analyze the neurite extension, the PC12 cells were firstly assembled into spheroids with a diameter in the range of 200–400 μm. We then seeded the spheroids on top of the aligned fibers in the tri-layer construct and used the diode laser to irradiate the construct at a power density of 1.0 W/cm^2 for 6 s and repeated six times at an interval of 2 hours. After incubation for 7 days, the cells were stained with Tuj1 marker. Figure 6, B and C, shows fluorescence micrographs of the neurites extending from the spheroids in the absence and presence of laser irradiation, respectively. In both groups, the neurites tended to extend along the alignment of the fibers, indicating the contact guidance of the aligned fibers underneath. From Figure 7, the neurites were much greater in terms of both average and the longest lengths, relative to the control group, when they extended from the spheroids in the presence of laser irradiation. This observation indicates that the NGF released upon photothermal heating significantly improved neurite extension. When the spheroids were cultured on the tri-layer construct with no NGF loaded in the PCM particles, no neurite extension was observed even under the same pattern of laser irradiation (Figure S12).

Taken together, we have successfully demonstrated the integration of NGF-loaded PCM particles with electrospun fibers for potential application in controlled release and neural tissue engineering. Upon increasing the local temperature to slightly pass the melting point of the PCM microparticles in the scaffold through photothermal heating, biological effectors can be released in a pulsatile mode with well-preserved bioactivity. Besides, the pulsatile release mode is instrumental in supplying fresh biological effectors to the tissue regeneration microenvironment. For potential *in vivo* nerve regeneration, by moving the laser spot on the nerve guidance conduit along the neurite outgrowth direction, it will be feasible to continuously trigger the release of neurotrophins into the nerve regeneration space. This method offers a new way for the on-demand release of growth factors towards tissue engineering.

3. Conclusion

We have demonstrated the fabrication of a temperature-dependent system for the controlled release of biological effectors. This system is based upon microparticles that were generated using coaxial electrospray to directly encapsulate the payload(s) inside a PCM matrix. Various types of payloads could be readily encapsulated in the PCM microparticles. Owing to the reversible phase change associate with PCM, the payload could be released in a pulsatile mode through multiple on/off heating cycles. By sandwiching the PCM microparticles (co-loaded with NGF and a NIR dye) between two layers of electrospun fibers, the NGF could be released on-demand by triggering with photothermal heating to stimulate the extension of neurites from spheroids of PC12 cells. This simple and versatile system can be readily applied to a variety of biomedical applications by switching to different combinations of PCM, biological effector, and scaffolding material.

4. Experimental Section

Chemicals and materials: Dulbecco's Modified Eagle's medium (DMEM), fetal bovine serum (FBS), new born calf serum, horse serum, phosphate buffered saline (PBS), and Neurite Outgrowth Kit were all purchased from Thermo Fisher Scientific. All other chemicals and materials were ordered from Sigma-Aldrich.

Fabrication of the microparticles: The coaxial electrospray setup is shown in Figure 1A. In a typical process, the PCM (a mixture of lauric acid and stearic acid at a mass ratio of 8:2) was dissolved in a mixture of ethanol and dichloromethane (20:80 by vol.) at a concentration of 20% and supplied as the outer solution. The payload was dissolved in 0.5 wt.% aqueous gelatin solution and used as the inner solution. After loading these two immiscible solutions into two syringes, we set the feeding rates of the outer and inner solutions to 3.0 mL/h and 1.0 mL/h, respectively. We examined

three different types of payloads: Rhodamine B (RB), fluorescein isothiocyanate labelled bovine serum albumin (FITC-BSA), and horseradish peroxidase (HRP). The high voltage applied to the coaxial spinneret was set to 25 kV. A piece of aluminum foil or glass slide was used as the collector. The as-obtained particles were characterized using both optical microscopy and fluorescence microscopy. The morphology of the particles loaded with FITC-BSA was further analyzed using scanning electron microscopy (SEM). The distribution of the payload in the particles was characterized using laser scanning confocal microscopy. We used the PCM solution as the outer solution and RB in 0.5 wt.% aqueous gelatin as the inner solution for electrospray. The as-obtained particles were imaged using a laser scanning confocal microscope (Zeiss 700). The encapsulation contents of the payloads were determined by measuring the UV/vis spectra of the PCM particles dissolved in ethanol, followed by quantification using the corresponding calibration curves.

Release of payloads from the microparticles upon heating: The particles containing a payload were dispersed in 1.0 mL of deionized water (Milli-Q, 18.2 MΩ cm) in a 1.5 mL centrifuge tube. The tube was immersed in a water bath set to the designated temperature (37 or 40 °C) and heated for different periods of time. For continuously heating, at intervals, 100 μL of the solution was collected to measure the released content. For the heating/cooling cycle measurement, at intervals, the tube was taken out and immediately cooled with an ice bath, followed by centrifugation at 12,000 rpm for 5 min. The supernatant was taken out to determine the released content, and then the precipitates were re-suspended with deionized water for further heating in the water bath. The absorbance at 560 nm of the released RB was measured using a microplate reader. The fluorescence intensity of the released FITC-BSA was measured using a microplate reader (λ_{ex} = 490 nm, λ_{em} = 525 nm). For the measurement of HRP released from the particles, long term heating at 40 °C would affect the enzymatic activity, so the samples were only heated at 40 °C for 3 min and then immersed in an ice bath. The heating and cooling cycles were repeated several times. The sample heated at 37 °C served as a control. The release content of HRP was determined by measuring the absorbance at 403 nm, followed by quantification using the calibration curve. To measure the enzymatic activity, 100 μL of

TMB substrate solution was added into the dilution of the released HRP at a concentration of 0.25 nM. Subsequently, the absorbance of the blue-colored product (peaked at 650 nm) was monitored continuously with 30 s intervals for 10 min. After adding aqueous HCl to stop the reaction after 20 min, we obtained the absorbance of the yellow-colored product at 450 nm, and the enzymatic activity was calculated by comparing with the absorbance obtained from the reaction with native HRP. Triplicate samples in each group were used for the release study.

Release of payloads from the microparticles upon photothermal heating: To demonstrate the ability of releasing payloads from PCM particles by photothermal heating, we co-loaded indocyanine green (ICG) into the particles as a near-infrared (NIR) absorber. The light-responsive release of payloads from the particles was evaluated by exposing the particles to a CW diode laser at 808 nm. Prior to the releasing test, the photothermal effect of the ICG-loaded PCM particles was evaluated. In this case, glass coverslips were employed as collectors for the electrosprayed particles. Under the irradiation of laser at different power densities, the rise in temperature of the dry particles was recorded as a function of the irradiation time using an infrared camera. The coverslips were also rinsed with deionized water, and the irradiation time that is needed to increase the temperature of the PCM particles to its melting point was obtained. For light-responsive releasing of the encapsulated payloads, the particles deposited on a glass coverslip was immersed in 1.0 mL of deionized water and then exposed to the diode laser for five rounds of on/off cycles. After laser irradiation in each round, the well plate was cooled with an ice bath, and 100 μL of the solution was collected to measure the released content of the payload. All the experiments with laser irradiation were performed at room temperature. The release of payloads from the particles in the absence of laser irradiation served as a control. The enzymatic activity of the released HRP was measured with the same method as described above. Triplicate samples in each group were used for the release study.

In vitro cytotoxicity of the microparticles: The cytotoxicity of the microparticles was evaluated using cell counting kit-8 (CCK-8) assay and NIH-3T3 cells. NIH-3T3 cells were seeded in the wells of a 24 well plate at a density of 2.0×10^4 cells per well and cultured in DMEM supplemented with

10% FBS in a cell culture chamber held at 37 ^{o}C. After 24 h, the cells were co-incubated with the particles at concentrations ranging from 2–1000 μg/mL. After incubation for another 24 h, the cells were washed with PBS, and CCK-8 reagent (10%) in culture medium was added into each well. After 4 h of incubation, the 24-well plate was shaken for 15 min, and then the absorbance of the supernatant at 450 nm was measured using a microplate reader. The cells incubated in the pristine culture medium served as a control.

Fabrication of the tri-layer construct: The tri-layer construct was fabricated through an integration of the electrospinning and electrospray processes. For electrospinning, the polymer solution (10 wt.%) was prepared by dissolving poly(ε-caprolactone) (PCL) in a mixture of dichloromethane and dimethylformaldehyde at a volume ratio of 80:20. Meanwhile, PCM (a mixture of lauric acid and stearic acid at a mass ratio of 8:2) was dissolved in a mixture of ethanol and dichloromethane (20:80 by vol.) at a concentration of 20%. The PCL solution was electrospun at a feeding rate of 1.0 mL/h through a blunt needle using a traditional electrospinning setup with a rotating mandrel as the collector. The voltage was set to 15 kV. Aligned PCL fibers were collected on the mandrel at a rotating speed of 1000 rpm for 2 h. The rotating speed of the mandrel was then reduced to 200 rpm. The PCL solution was replaced with the PCM solution, and microparticles were electrosprayed from a blunt needle under a voltage of 25 kV. Afterwards, the electrospinning setup was used again to deposit a layer of PCL random fibers onto the mandrel for 2 h. Constructs integrated with different amounts of PCM particles were fabricated by changing the electrospray durations for 5, 10, and 20 min, respectively, to evaluate the cytotoxicity of the tri-layer construct towards NIH-3T3 cells. We also integrated the PCM particles containing nerve growth factor (NGF) between the two layers of fibers. In the electrospray process, the blunt needle was replaced with a dual-capillary needle, and the PCM solution was used as the outer fluid while NGF and ICG dissolved in a 0.5 wt.% aqueous gelatin solution at a concentration of 50 μg/mL and 1 mg/mL, respectively, was used as the inner fluid. The feeding speeds of the outer and inner fluids were set to 3.0 mL/h and 1.0 mL/h, respectively. The tri-layer construct containing NGF was broken in liquid nitrogen along the

direction of alignment for the aligned fibers, and the cross-section was imaged using a scanning electron microscope. The tri-layer construct was also frozen-embedded in the optimal cutting temperature compound, sectioned using a cryostat (CryoStar NX70), and then analyzed using an optical microscope.

Triggered release of NGF from tri-layer construct: The tri-layer construct was cut into disc with a diameter of 1.5 cm, fixed on a glass coverslip, and then affixed to the bottom of a well in a 24 well plate with a small dab of medical adhesive. Afterwards, 1.0 mL of deionized water was added into each well. The plates were sealed and placed at room temperature. To trigger the release of the NGF, all the well plates were either put in a chamber held at 40 °C for 3 min or exposed to the diode laser at a power density of 1.0 W/cm^2 for 6 s, and this procedure was repeated once every day for 7 days. The content of NGF released from the tri-layer construct was measured using NGF Elisa following the manufacture's protocol.

Neurite outgrowth under the release of NGF: We investigated the neurite outgrowth from PC12 cells under stimuli-release of NGF from the tri-layer construct upon direct heating or photothermal heating. For direct heating, PC12 cells were seeded at the bottom of a well in a 24-well plate and cultured in 1.0 mL of DMEM containing 10% horse serum and 5% new born calf serum. After incubation for 24 h, the culture medium was replaced with 600 μL of DMEM containing 1% horse serum. The tri-layer construct was cut into a disc with a diameter of 0.65 cm and placed in the apical chamber of a Corning HTS Transwell^{TM} 24-well insert. Then, the system was placed in the well of the 24-well plate, and 100 μL of DMEM containing 1% horse serum was added into the chamber of the insert. Afterwards, the well plate was heated in a chamber at 40 °C for 3 min and then incubated in the cell culture chamber held at 37 °C. For the control group, PC12 cells were incubated in 700 μL of culture medium supplemented with 20 ng/mL of NGF. During the incubation, at day 2, 4, and 6, the well plate was also heated in the chamber at 40 °C for 3 min, respectively.

For photothermal heating, we firstly measured the amount of NGF cumulatively released from the tri-layer construct. A tri-layer construct containing NGF was cut into a disc with a diameter of 0.65 cm and placed in the apical chamber of a 24-well insert. The system was then placed in a well of a 24-well plate. Afterwards, 700 μL of DMEM containing 1% horse serum was added into each well. The tri-layer construct was then exposed to the diode laser at a power density of 1.0 W/cm^2 for 6 s, and this irradiation procedure was repeated at day 2, 4, and 6, respectively. At day 7, the cumulatively released amount of NGF was measured using NGF Elisa. The well plate in the absence of laser irradiation served as a control. The medium containing the released NGF was then collected for incubation of PC12 cells for 7 days to examine the activity of the released NGF.

We then investigated the neurite outgrowth from PC12 cells under stimuli-release of NGF from the tri-layer construct upon photothermal heating using the same method as described for direct heating. The constructs were exposed to the diode laser at a power density of 1.0 W/cm^2 for 6 s, and the well plate was then incubated in the cell culture chamber held at 37 °C. During the incubation, at day 2, 4, and 6, the irradiation procedure was repeated, respectively.

At day 7 of incubation, the PC12 cells were stained with the Neurite Outgrowth Kit following the manufacture's protocol and then analyzed under a fluorescence microscope. The average and the longest neurite lengths were quantitatively analyzed from the fluorescence micrographs. The percent of cells bearing neurites—the neurites length is greater than or equal to the diameter of the cell body—was determined by counting 150 cells in randomly selected fields of the micrographs. Triplicate samples in each group were used for the study.

Furthermore, we investigated the neurite outgrowth from the PC12 cells directly cultured on the tri-layer construct under the effect of the NGF released upon photothermal heating. A tri-layer construct with a diameter of 1.2 cm was fixed onto a glass coverslip with the aligned fiber on the top, and then affixed to the bottom of a well in a 24 well plate. PC12 multicellular spheroids with a diameter in the range of 200–400 μm were formed by culturing the cells in laminin-coated flask for

8–10 days and then seeded on the tri-layer construct. After incubation for 24 h, the culture medium was replaced with DMEM containing 1% horse serum, and then the tri-layer construct was exposed to the diode laser at a power density of 1.0 W/cm^2 for 6 s and repeated 6 times at an interval of 2 hours. The tri-layer construct with no laser irradiation served as a control. After 7 days, the neurites extruding from the PC12 spheroids were immunostained with anti-βIII tubulin antibody, and the spheroids were imaged under a fluorescence microscope. The average and the longest neurite lengths were quantitatively analyzed from the fluorescence micrographs using ImageJ software. Triplicate samples in each group were used for the study.

Statistical Analysis. All the results are presented in the form of mean ± standard deviation, with "n" indicating the number of samples per group. Statistical analysis was performed using the Student's t test in SPSS. Differences were considered statistically significant when $P < 0.05$.

Supporting Information

Supporting Information is available from the Wiley Online Library or from the author.

Acknowledgements

This work was supported in part by a grant from the National Institutes of Health (R01 EB020050) and startup funds from the Georgia Institute of Technology.

References

[1] N. A. Kotov, J. O. Winter, I. P. Clements, E. Jan, B. P. Timko, S. Campidelli, S. Pathak, A. Mazzatenta, C. M. Lieber, M. Prato, *Adv. Mater.* **2009**, *21*, 3970.

[2] M. R. Abidian, D. C. Martin, *Adv. Funct. Mater.* **2009**, *19*, 573.

[3] P. Fattahi, G. Yang, G. Kim, M.R. Abidian, *Adv. Mater.* **2014**, *26*, 1846.

[4] R. V. Bellamkonda, S. B. Pai, P. Renaud, *MRS Bull.* **2012**, *37*, 557.

[5] G. Malliaras, M. R. Abidian, *Adv. Mater.* **2015**, *27*, 7492.

[6] C. Hassler, T. Boretius, T. Stieglitz, *J. Polym. Sci. Pol. Phys.* **2011**, *49*, 18.

[7] L. G. Griffith, G. Naughton, Science 2002, 295, 1009.

[8] K. J. Rambhia, P. X. Ma, *J. Controlled Release* **2015**, *219*, 119.

[9] Y. Brudno, D. J. Mooney, *J. Controlled Release* **2015**, *219*, 8.

[10] M. A. C. Stuart, W. T. S. Huck, J. Genzer, M. Muller, C. Ober, M. Stamm, G. B. Sukhorukov, I. Szleifer, V. V. Tsukruk, M. Urban, F. Winnik, S. Zauscher, I. Luzinov, S. Minko, *Nat. Mater.* **2010**, *9*, 101.

[11] M. S. Yavuz, Y. Cheng, J. Chen, C. M. Cobley, Q. Zhang, M. Rycenga, J. Xie, C. Kim, K. H. Song, A. G. Schwartz, *Nat. Mater.* **2009**, *8*, 935.

[12] M. F. Chung, K. J. Chen, H. F. Liang, Z. X. Liao, W. T. Chia, Y. Xia, H. W. Sung, *Angew. Chem. Int. Ed.* **2012**, *51*, 10089.

[13] G. D. Moon, S. W. Choi, X. Cai, W. Li, E. C. Cho, U. Jeong, L. V. Wang, Y. Xia, *J. Am. Chem. Soc.* **2011**, *133*, 4762.

[14] S. Laurent, D. Forge, M. Port, A. Roch, C. Robic, L. Vander Elst, R. N. Muller, *Chem. Rev.* **2008**, *108*, 2064.

[15] X. Zhao, J. Kim, C. A. Cezar, N. Huebsch, K. Lee, K. Bouhadir, D. J. Mooney, *Proc. Natl. Acad. Sci. U. S. A.* **2011**, *108*, 67.

[16] J. T. Santini, M. J. Cima, R. Langer, *Nature* **1999**, *397*, 335.

[17] M. R. Abidian, D. H. Kim, D. C. Martin, *Adv. Mater.* **2006**, *18*, 405.

[18] N. Fomina, C. McFearin, M. Sermsakdi, O. Edigin, A. Almutairi, *J. Am. Chem. Soc.* **2010**, *132*, 9540.

[19] S. W. Choi, Y. Zhang, Y. Xia, *Angew. Chem. Int. Ed.* **2010**, *49*, 7904.

[20] D. C. Hyun, P. Lu, S. I. Choi, U. Jeong, Y. Xia, *Angew. Chem. Int. Ed.* **2013**, *52*, 10468.

[21] D. C. Hyun, N. S. Levinson, U. Jeong, Y. Xia, *Angew. Chem. Int. Ed.* **2014**, *53*, 3780.

[22] J. Liu, C. Detrembleur, M. C. De Pauw-Gillet, S. Mornet, L. Vander Elst, S. Laurent, C. Jérôme, E. Duguet, *J. Mater. Chem. B* **2014**, *2*, 59.

[23] Y. Yuan, N. Zhang, W. Tao, X. Cao, Y. He, *Renew. Sustainable Energy Rev.* **2014**, *29*, 482.

[24] Y. Yanping, T. Wenquan, C. Xiaoling, B. Li, *J. Chem. Eng. Data* **2011**, *56*, 2889.

[25] Z. Zhang, Y. Yuan, N. Zhang, X. Cao, *J. Chem. Eng. Data* **2015**, *60*, 2495.

[26] P. Zhao, Q. Yue, H. He, B. Gao, Y. Wang, Q. Li, *Appl. Energy* **2014**, *115*, 483.

[27] S. Shen, C. Zhu, D. Huo, M. Yang, J. Xue, Y. Xia, *Angew. Chem. Int. Ed.* **2017**, *129*, 8927.

[28] C. Zhu, P. Pradhan, D. Huo, J. Xue, S. Shen, K. Roy, Y. Xia, *Angew. Chem. Int. Ed.* **2017**, *56*, 10399.

[29] C. Zhu, D. Huo, Q. Chen, J. Xue, S. Shen, Y. Xia, *Adv. Mater.* **2017**, *doi: adma.201703702*.

[30] P. Selcan Gungor-Ozkerim, T. Balkan, G. T. Kose, A. Sezai Sarac, F. N. Kok, *J. Biomed. Mater. Res. Part A* **2014**, *102*, 1897.

[31] H. Lai, C. Kuan, H. Wu, J. C. Tsai, T. Chen, D. J. Hsieh, T. Wang, *Acta Biomater.* **2014**, *10*, 4156.

[32] P. Jayaraman, C. Gandhimathi, J. R. Venugopal, D. L. Becker, S. Ramakrishna, D. K. Srinivasan, *Adv. Drug Deliv. Rev.* **2015**, *94*, 77.

[33] S. Qi, D. Craig, *Adv. Drug Deliv. Rev.* **2016**, *100*, 67.

[34] K.-H. Roh, D. C. Martin, J. Lahann, *Nat. Mater.* **2005**, *4,* 759.

[35] P. Fattahi, A. Borhan, M. R. Abidian, *Adv. Mater.* **2013**, *25*, 4555.

[36] Y. Jing, Y. Zhu, X. Yang, J. Shen, C. Li, *Langmuir* **2010**, *27*, 1175.

[37] P. Davoodi, F. Feng, Q. Xu, W. Yan, Y. W. Tong, M. P. Srinivasan, V. K. Sharma, C. Wang, *J. Controlled Release* **2015**, *205*, 70.

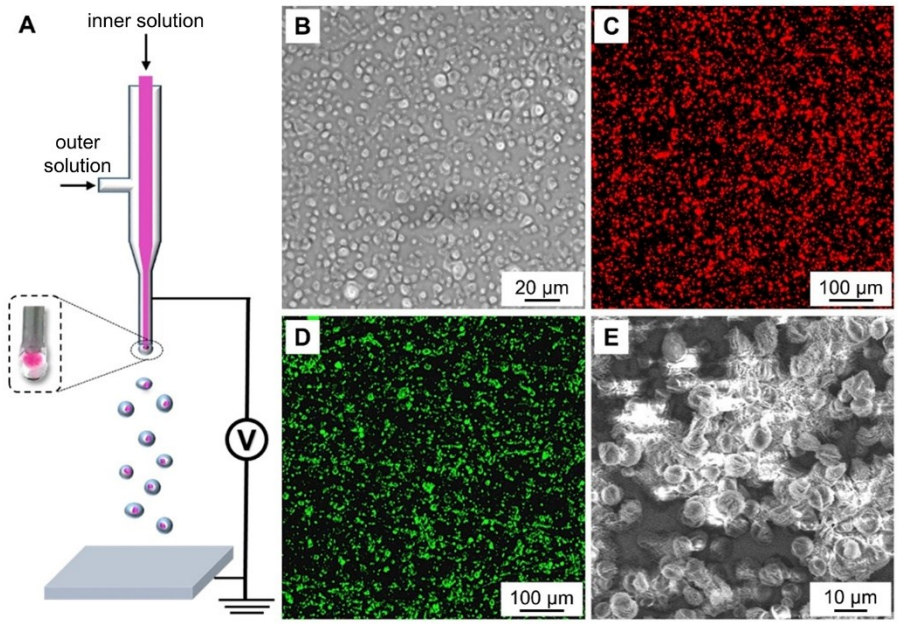

Figure 1. (A) Schematic illustration of the coaxial electrospray setup used for the fabrication of PCM microparticles containing a payload in the core region. (B, C) Optical and fluorescence micrographs, respectively, of the microparticles loaded with Rhodamine B. (D, E) Fluorescence micrograph and SEM image, respectively, of the microparticles loaded with FITC-BSA.

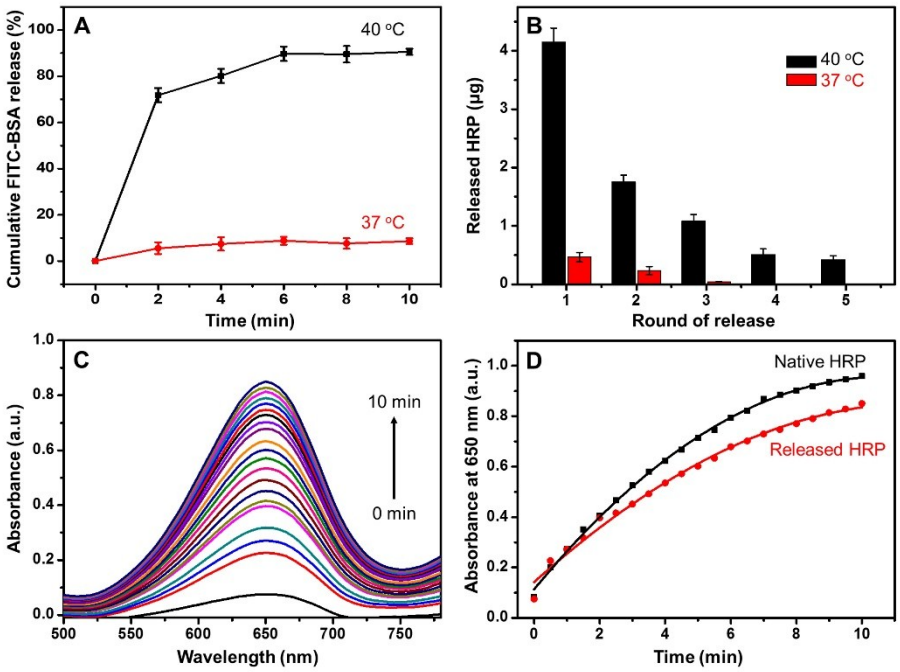

Figure 2. Release of various types of payloads from the PCM microparticles. (A) Cumulative release of FITC-BSA from the particles upon continuously heating at 37 °C and 40 °C, respectively (n = 3). (B) Amounts of HRP released from the particles after heating at 37 °C and 40 °C for 3 min, respectively, and repeated for five rounds (n = 3). (C) UV/vis absorption spectra of the blue-colored product derived from the reaction between TMB and the HRP released from the particles by heating at 40 °C for 3 min. The spectra were recorded for 10 min at an interval of 30 s. (D) Typical plot of the time-dependent absorbance changes of the blue-colored product at 650 nm derived from the reaction between TMB and the native or thermally released HRP, respectively. At the same concentration of HRP, the slower initial reaction rate constant, which is the slope of the initial linear region, suggests a lower enzymatic activity.

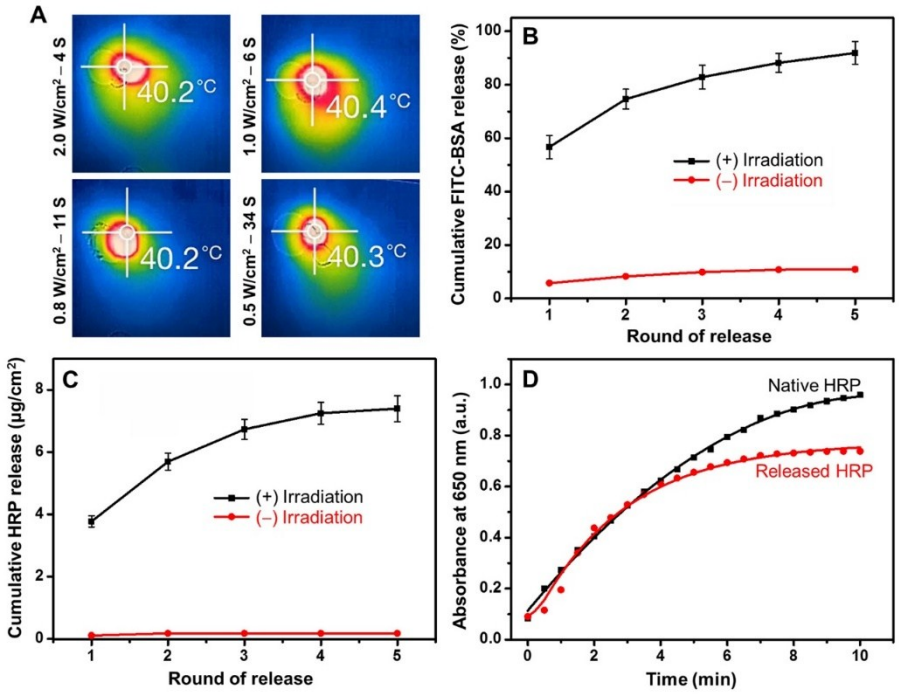

Figure 3. Photothermal effect and the release of payloads from the PCM microparticles. Indocyanine green (ICG) was co-loaded into the particles as a NIR absorber. (A) Infrared images showing the rise of temperature to slightly pass the melting point of the PCM upon irradiation with the diode laser at different power densities for different periods of time. Cumulative release of (B) FITC-BSA and (C) HRP from the particles upon laser irradiation at a power density of 1.0 W/cm^2, respectively (n = 3). (D) Typical plot of the time-dependent absorbance changes of the blue-colored product at 650 nm derived from the reaction between TMB and the native or photothermally released HRP, respectively.

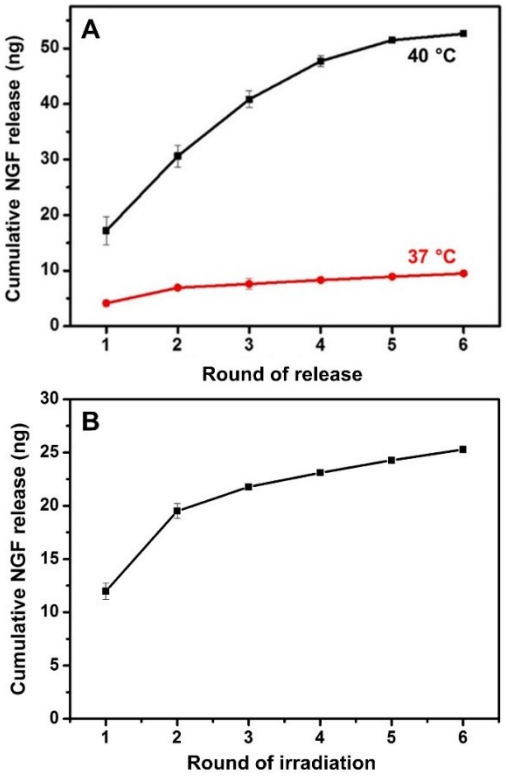

Figure 4. The cumulative release profiles of NGF from the tri-layer construct upon (A) direct heating at 37 °C and 40 °C, respectively, for 3 min and repeated six rounds (n = 3) and (B) photothermal heating upon laser irradiation for 6 s at a power density of 1.0 W/cm^2 and repeated six rounds (n = 3).

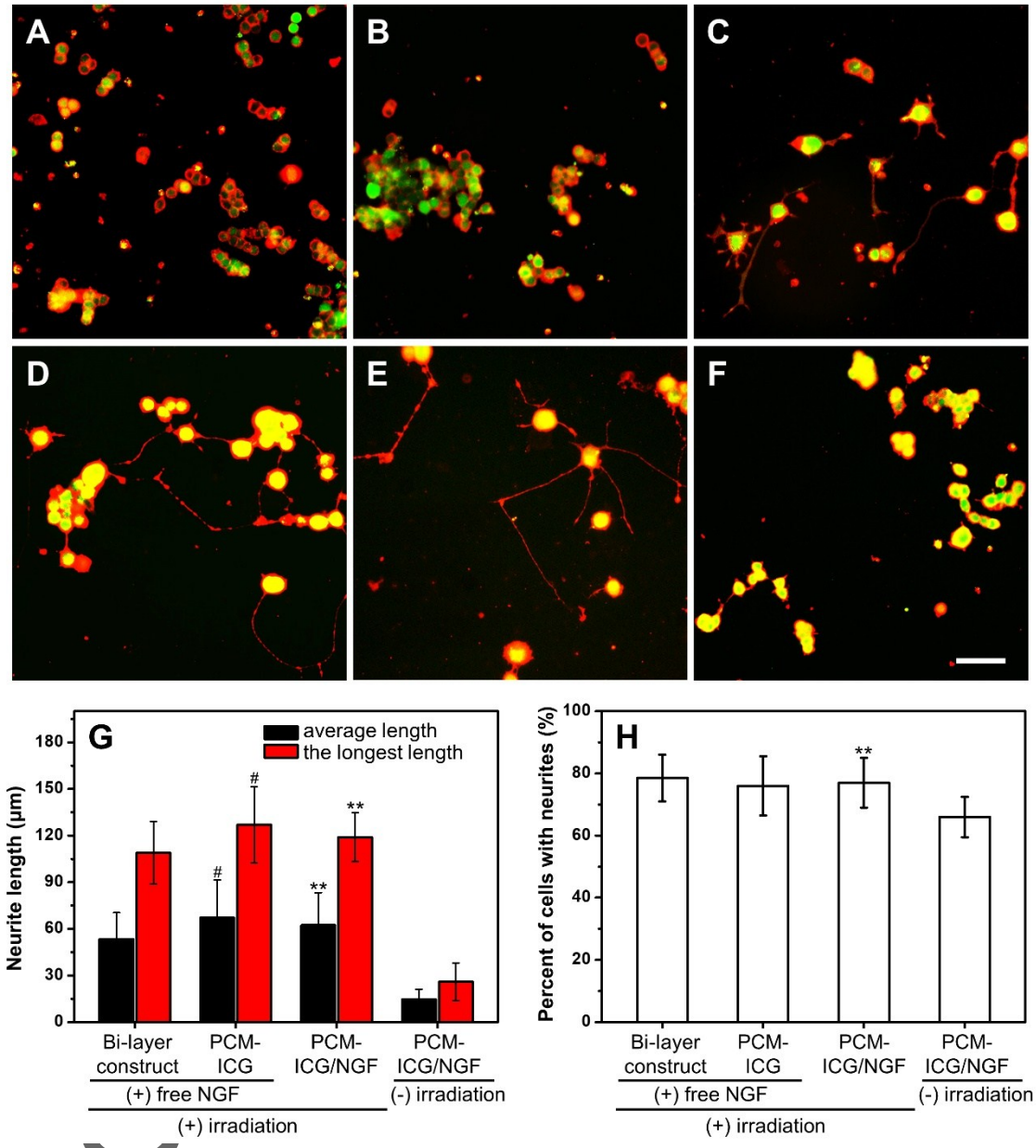

Figure 5. Fluorescence images of the PC12 cells after incubation for 7 days under the effect of different constructs upon laser irradiation: (A) bi-layer construct with one layer consisting of random fibers and the other layer consisting of random fibers, (B) tri-layer construct sandwiched with PCM microparticles containing ICG only (PCM-ICG), (C) bi-layer construct with free NGF supplemented in the culture medium, (D) tri-layer construct (PCM-

ICG) with free NGF supplemented in the culture medium, and (E) tri-layer construct sandwiched with PCM microparticles containing both ICG and NGF (PCM-ICG/NGF). (F) Fluorescence image of the PC12 cells after incubation for 7 days under the effect of tri-layer construct sandwiched with PCM microparticles containing both ICG and NGF (PCM-ICG/NGF) in the absence of laser irradiation. The plasma membrane was stained in red while the cell body was stained in green using a Neurite Outgrowth Kit. Scale bar = 50 μm. (G) The average and the longest lengths of neurites extending from the PC12 cells, and (H) the percent of cells bearing neurites. Measurements were taken from 3 sets of 150 cells for each group. The three sets were from three representative experiments. $^{\#}P < 0.05$ significantly higher than the group of bi-layer construct; by Student's t test. $^{**}P<0.01$ compared with the group with no laser irradiation, by Student's t test.

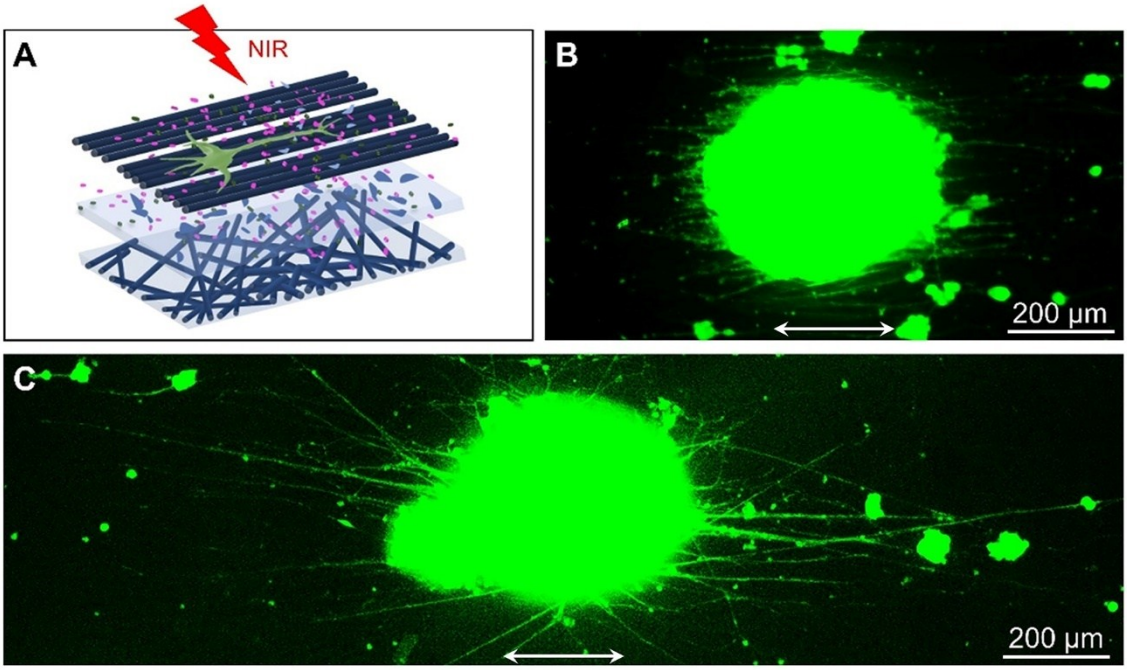

Figure 6. (A) Schematic showing the neurite outgrowth from spheroids of PC12 cells incubated on the tri-layer construct under the effect of NGF released from the sandwiched PCM particles upon photothermal heating with the diode laser. Fluorescence micrographs of the typical neurite fields extending from the spheroids when directly cultured on the tri-layer construct in the (B) absence and (C) presence of laser irradiation, respectively. The neurites were stained with Tuj1 marker (green). The arrows indicate the alignment directions of the fibers.

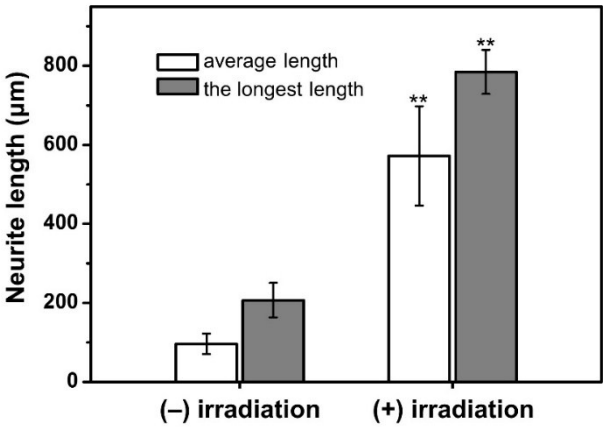

Figure 7. The average and the longest lengths of neurites extending from the spheroids of PC12 cells when directly cultured on the tri-layer construct with/without laser irradiation. ***P*<0.01 when compared with the group without laser irradiation, by Student's t test (n = 3).

Author/s:
Xue, J;Zhu, C;Li, J;Li, H;Xia, Y

Title:
Integration of Phase-Change Materials with Electrospun Fibers for Promoting Neurite Outgrowth under Controlled Release.

Date:
2018-04-11

Citation:
Xue, J., Zhu, C., Li, J., Li, H. & Xia, Y. (2018). Integration of Phase-Change Materials with Electrospun Fibers for Promoting Neurite Outgrowth under Controlled Release.. Adv Funct Mater, 28 (15), pp.1705563-. https://doi.org/10.1002/adfm.201705563.